Regenerative Therapy 28 (2025) 438–450

Contents lists available at ScienceDirect

Regenerative Therapy

journal homepage: http://www.elsevier.com/locate/reth

Original Article

Modified bFGF targeting connective tissue growth factor in the injured microenvironment improved cardiac repair after chronic myocardial ischemia

Shuwei Sun [a, 1], Fengzheng Zhu [b, 1], Qingling Xu [a, 1], Xianglin Hou [c], Weihong Nie [d], Kaiyan Su [a], Li Wang [e], Zhuo Liu [a], Tao Shan [a, **], Chunying Shi [a, *]

[a] Department of School of Basic Medicine, Qingdao University, Qingdao, Shandong Province 266071, China
[b] Department of Cardiac Surgery, The Affiliated Hospital of Qingdao University, 16 Jiangsu Road, Qingdao, Shandong Province 266000, China
[c] State Key Laboratory of Molecular Developmental Biology, Institute of Genetics and Developmental Biology, Chinese Academy of Sciences, Beijing, 100190, China
[d] Department of Medicine, Qingdao University, Qingdao, Shandong Province 266071, China
[e] Department of Neurology, The Affiliated Hospital of Qingdao University, 16 Jiangsu Road, Qingdao, Shandong Province 266000, China

ARTICLE INFO

Article history:
Received 4 December 2024
Received in revised form
27 December 2024
Accepted 10 January 2025

Keywords:
Targeted delivery
Connective tissue growth factor
Basic fibroblast growth factor
Myocardial ischemia
Cardiac remodeling

ABSTRACT

Myocardial infarction (MI) was a cardiovascular emergency that led to heart failure, arrhythmia, and sudden death. Basic fibroblast growth factor (bFGF) was revealed to promote angiogenesis and protect cardiomyocytes against ischemic injury. But conventional delivery of bFGF in an uncontrolled manner was inefficient and diffusive, limiting its application in MI therapy. Currently, stimuli-responsive drug delivery is emphasized in tissue regeneration. The present study constructed a CFBP-bFGF recombinant protein, which could specifically target upregulated connective tissue growth factor (CTGF) and release bFGF in ischemic myocardium. In a rat model with MI, intravenous administration of CFBP-bFGF significantly accumulated in ischemic myocardium by targeting with CTGF. The responsive release of CFBP-bFGF effectively enhanced blood vessel regeneration, decreased cardiomyocyte apoptosis, and improved cardiac function recovery. In addition, the molecular mechanism was further explored by RNA sequencing and transcriptome analysis. Besides activating the pathways and genes related to angiogenesis and cardiac protection, CFBP-bFGF also decreased the expression of fibrosis-related pathways and genes, such as TGF-β. These results demonstrated that the CTGF-responsive CFBP-bFGF was effective for targeting release that promoted the functional recovery of MI.

1. Introduction

Myocardial infarction (MI) is the leading cause of morbidity and mortality globally [1]. Following MI, blood flow obstruction results in the loss of cardiomyocytes, the progressive structural remodeling, which ultimately develops into heart failure [2]. Therefore, timely revascularization, such as pharmacological therapies, surgical interventions, and coronary artery bypass grafting, were conventional treatment treatments for MI. In recent years, angiogenic growth factors have been shown to effectively increase blood perfusion in the ischemic microenvironment, which would be potential strategies for further MI therapy [3].

Among these growth factors, basic fibroblast growth factor (bFGF) plays a more extensive role. It was reported bFGF could promote the proliferation, and migration of endothelial cells and vascular smooth muscle cells *in vitro* and *in vivo*, which increased regional myocardial blood flow and contributed to reconstruct a mature blood vessel network in different animal MI models [4]. In addition, bFGF could also protect cardiomyocyte survival [3,5]. However, in clinical trials, a single intracoronary bFGF infusion was shown to reduce angina symptoms but could not enhance

* Corresponding author.
** Corresponding author.
E-mail addresses: sunshuwei0726@163.com (S. Sun), 2251783896@qq.com (F. Zhu), xql200002@163.com (Q. Xu), houxianglin816@126.com (X. Hou), whongnie@163.com (W. Nie), sky2262023@163.com (K. Su), wang_l2023@163.com (L. Wang), 17639722275@163.com (Z. Liu), shantao022@163.com (T. Shan), schy1116@163.com (C. Shi).

Peer review under responsibility of the Japanese Society for Regenerative Medicine.

[1] These authors contributed equally to this work.

https://doi.org/10.1016/j.reth.2025.01.006

myocardial perfusion [6]. That might be due to the rapid diffusion and short half-life of bFGF in the body, directly causing insufficient regional concentration in ischemic myocardium [7]. Therefore, how to increase the regional concentration of bFGF was critical for its further clinical application [8,9].

Recently, a stimuli-responsive release system was emphasized for the delivery of growth factors that significantly facilitated tissue regeneration. After tissue injury, a series of specific molecules were upregulated in pathological environments as cues for targeting delivery. In our previous studies, a specific ischemic myocardium targeting- IMT-VEGF was designed, which recognized the cardiac troponin I (cTnI) to guide VEGF to ischemic myocardium in acute ischemia/reperfusion injury animal models [10]. cTnI was a structural protein responsible for myocardial contraction. Following MI, cTnI was released into a hypoxic environment immediately, then slowly released into the blood, which served as a reliable diagnostic indicator a few hours after MI. Thus, cTnI was a useable targeting candidate for drug delivery of acute myocardial ischemic injury, but was not available in later stages, especially for repeated administration. As a result, new targeting candidates in ischemic myocardium were needed.

After MI, connective tissue growth factor (CTGF) was demonstrated to be gradually upregulated in ischemic myocardium and participated in subsequent cardiac fibrosis. In a previous study, a specific CFBP peptide-CDAGRKQKC was confirmed to typically bind with CTGF by *in vivo* phage display [11]. Then we constructed a recombinant CFBP-bFGF fused protein, the CFBP-bFGF could target the injured brain and skin which highly expressed CTGF through intravenous injection [12]. As CTGF gradually increased in ischemic myocardium, whether CFBP-bFGF could identify CTGF and preserve the regional concentration of bFGF in the injured site was unknown. In the present study, the bioactivity, cardioprotective effect, and targeting efficiency of CFBP-bFGF were detected *in vitro* and *in vivo*; then the cardiac repair effect of CFBP-bFGF was investigated in rats model of MI; finally, the molecular mechanism of CFBP-bFGF was explored by RNA sequencing and transcriptome analysis (see Scheme 1).

2. Materials and methods

2.1. Preparation of CFBP-bFGF

The CFBP-bFGF coding gene was synthesized and inserted into the pET28a vector, which was subsequently transferred to BL21^{+} *E. coli* (DP118–02, TIANGEN BIOTECH, Beijing) for overnight amplification. At 30 ℃, the expression was induced with isopropyl β-*d*-thiogalactoside (IPTG) at a final concentration of 1 mM for 5h, and the *E. coli* were collected by centrifugation and crushed by ultrasound. The target protein was purified from the supernatant by Nickel column using the AKATA Primer system (AKTA pure 25, GE), which was eluted with gradient imidazole. Finally, the purity of recombinant proteins was detected by sodium dodecyl sulfate-polyacrylamide gel electrophoresis and Western blot.

2.2. Bioactivity assay of CFBP-bFGF and bFGF

The biological activity of CFBP-bFGF was evaluated by promoting the proliferation of human skin fibroblasts (HSFs). HSFs were seeded in 48-well plates at a density of 3000 cells/well. After the cells adhered, the medium supplemented with CFBP-bFGF and bFGF with the concentration gradients (0, 625 pM, 1250 pM, 2500 pM, 5000 pM) were added and incubated in 37 ℃, 95 % O_2, 5 % CO_2 incubator for 48h. Then 3-(4,5)-dimethylthiahiazo(-z-y1)-3,5-diphenytetrazoliumromide (MTT, M8180, Solarbio) was added into wells for 4h, and then DMSO (D8370, Solarbio) of 450 μL/well was added to incubate in the dark for 10min, and the optical density (OD) of the sample was detected by universal microplate spectrophotometer (CMax Plus) at 492 nm.

2.3. Establishment of oxygen-glucose deprivation/reoxygenation model (OGD/R model)

H9c2 cells were cultured with high-glucose DMEM containing 10 % fetal bovine serum (FBS) in a 37 ℃ incubator (95 % O_2 and 5 % CO_2). Then low-glucose DMEM containing 1 % FBS with different gradients (0, 3.125 nM, 6.25 nM, 12.5 nM) bFGF or CFBP-bFGF was replaced and incubated in an anoxic incubator (2 % O_2 and 98 % N_2) for 6h, then changed into complete medium and reoxygenated at 37 ℃ with 95 % O_2 and 5 % CO_2 for 18h. The survival rate of H9c2 cells was determined by MTT as described above.

2.4. Rodent models of myocardial infarction

All experimental procedures were carried out according to the local guidelines for the ethical use of animals and the National Institutes of Health's Guidelines for the Care and Use of Laboratory Animals (NIH publication 23–80, revised in 2011), and all protocols were approved by the Animal Care and Use Committee of Qingdao University (Approval No. QDU-AEC-2023365). Adult female Sprague–Dawley rats (210–240 g) (Jinan Pengyue Experimental Animal Breeding Co.) were randomly divided into three groups of 6 rats each group, which were the PBS group, bFGF group, and CFBP-

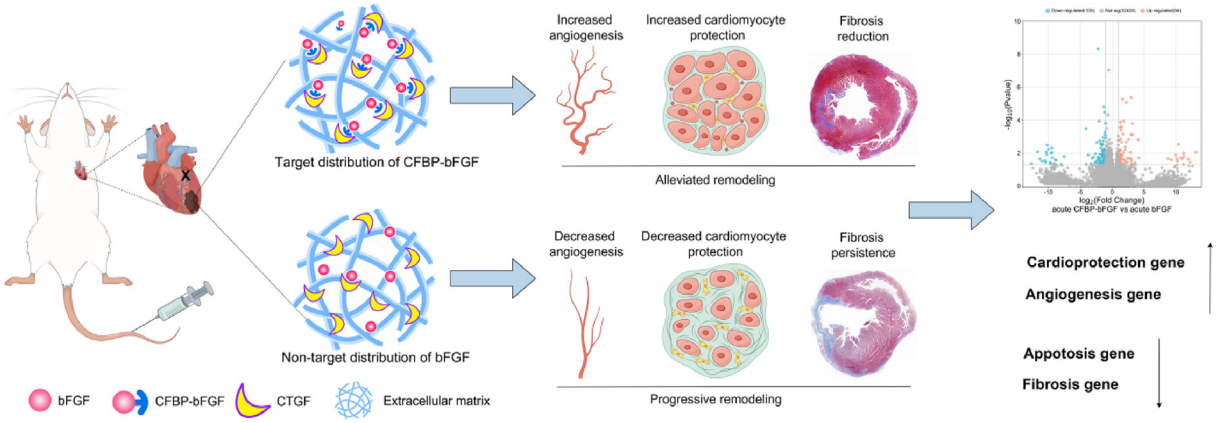

Scheme 1. Schematic illustration of responsive release of targeting CFBP-bFGF improved cardiac repair after chronic myocardial ischemia in rats.

bFGF group. Referring to previous studies, the rats were anesthetized by intraperitoneal injection of 50 mg/kg sodium pentobarbital, and the left chest was exposed and fixed on the operating table. Endotracheal intubation, mechanical ventilation, then thoracotomy in the left fourth costal space to ligate the left anterior descending artery. Finally, the thoracic cavity was closed, and postoperative ventilation was maintained until the rats regained consciousness. For the ELISA assay, the MI rats were intravenously injected with CFBP-bFGF (0.58 nmol, 0.05 mg/kg) and bFGF (0.58 nmol, 0.05 mg/kg) via the tail vein at 3 days, 1 week, and 2 weeks after MI. For animal experiments to evaluate the regenerative effects of CFBP-bFGF, the MI rats were intravenously injected with CFBP-bFGF (0.35 nmol, 0.03 mg/kg) and bFGF (0.35 nmol, 0.03 mg/kg) via the tail vein at 3 days, 1 week, 2 weeks, 3 weeks and 4 weeks after MI; at 4, 8 weeks after MI, Echocardiography was performed for cardiac function evaluation. The procedure of animal experiments is shown in Supplementary 1.

2.5. Tube formation assay

50 μL/well Matrigel matrix (356234, Corning) was added into the pre-cooled 96-well plate and placed in a 37 ℃ incubator for 45~60 min until the gel was cured. The HUVECs cell suspension (1×10^5 cells/well) was uniformly added into the wells pre-coated with Matrigel and divided into 3 groups: Control group (high glucose DMEM, 2 % FBS), bFGF group (high glucose DMEM, 2 % FBS, 50 ng/mL bFGF), CFBP-bFGF group (high glucose DMEM, 2 % FBS, 50 ng/mL CFBP-bFGF). The 96-well plates were then placed in an incubator. The tubular structures formed with HUVECs were observed by microscope and analyzed by ImageJ software plus Angiogenesis Analyzer tool.

2.6. Quantitative ELISA analysis of CFBP-bFGF in the ischemic myocardium and serum

The rats were intravenously injected with CFBP-bFGF (0.58 nmol, 0.05 mg/kg) and bFGF (0.58 nmol, 0.05 mg/kg) via the tail vein at 3 days, 1 week, and 2 weeks after MI. Ischemic myocardial tissue and serum samples were collected 6h post-administration for subsequent quantitative analysis of bFGF using an ELISA kit (EK0342, BOSTER). The experimental procedure was conducted according to the provided instructions.

2.7. Western blot

0.1 g ischemic myocardium tissue was taken, and 10 μL PMSF and 1 mL RIPA were added for protein extraction. After quantification, the proteins were separated by SDS-PAGE gel and transferred to the PVDF membrane. The antigen sites were blocked by 5 % skim milk powder, incubated at room temperature for 1~2h, and incubated at 4 ℃ in the corresponding primary antibody overnight: Anti-FGF-2 Rabbit pAb (1:1000, BS6432, Bioworld), Anti-CTGF (1:1000, BS-0743R, Bioss), Anti-Smad7 Rabbit pAb(1:1000, 860746, zenbio), Anti-TGF beta 1 Rabbit mAb(1:1000, HUABIO, HA721143), Anti-Smad3(1:2000, Abcam, ab40854), Anti-p-Smad3 Rabbit mAb(1:1000, zenbio, R22919), Anti-β-actin Rabbit pAb (1:10,000, AP0060, Bioworld), Anti-GAPDH Rabbit pAb (1:10,000, AP0066, Bioworld). After TBST cleaning, the membrane was placed in a secondary antibody: Goat Anti-Rabbit IgG (1:10,000, HA1001, HUABIO) of the same species as the primary antibody at room temperature for 1h, and the images were obtained with an ultra-sensitive chemiluminescence detection kit and automatic chemiluminescence image analysis system (Tanon-5200).

2.8. Cardiac function evaluation by echocardiography

Chest echocardiography was done under general anesthesia with 2 % isoflurane and 0.2 L/min oxygen at 4w and 8w after MI. After anesthesia, echocardiography was performed using an 18 MHz linear transducer of an animal cardiovascular ultrasound system (VINNO, V6Lab, China). The animal cardiovascular ultrasound system automatically calculated ejection fraction (EF), shortened fraction (FS), and left-ventricular M-mode echocardiography was used to measure left ventricular systolic diameter (LVDs), left ventricular end-diastolic diameter (LVDd), interventricular septum end-systolic thickness (IVSs) and left ventricular posterior wall thickness (LVPWd).

2.9. Histological analysis

After the animals were sacrificed, the chest cavity was opened and perfused with normal saline through the left ventricle. After the effluence became apparent, the heart was removed and transversely dissectioned. The upper part of the heart tissue sample was taken and fixed with 4 % paraformaldehyde for 48h. The tissue was gradient dehydrated with alcohol (50 %, 70 %, 90 %, 95 %), transparent with xylene, and the soft paraffin wax was incorporated at 55 ℃ for 2h, using the hard paraffin to repeat the process at 60 ℃. The embedded tissues were cut into 5 μm slices for hematoxylin and eosin staining (H&E) and Masson's trichrome staining.

2.10. Immunofluorescence staining

The paraffin sections were normally dewaxed to water, then 20 % fetal bovine serum (FBS) was used to block the non-specific antigen sites for 30 min, and then covered with primary antibodies: Anti-FGF-2 antibody (1:200, SC-74412, Santa Cruze), Anti-CTGF antibody (1:200, BS-0743R, Bioss), Anti-alpha smooth muscle Actin (α-SMA) antibody (1:500, AB124964, Abcam), Anti-von Willebrand Factor (vWF) antibody (1:500, AB6994, Abcam) and Anti-cardiac Troponin T (cTnT) antibody (1:500, AB8295, Abcam), Anti-Collagen I antibody (1:400, bs-10423R, Bioss), Vimentin Rabbit mAb (1:100, R22775, Zenbio) were added, and were bound overnight in the wet box at 4 ℃. After cleaning and re-sealing on the second day, Goat Anti-Rabbit IgG H&L (Alexa Fluor® 594) (1:400, AB150080, Abcam) or Goat Anti-Mouse IgG H&L(Alexa Fluor® 488) (1:400, AB150113, Abcam) with the same species as the primary antibody was added and placed at room temperature for 2h to form antigen-primary-secondary antibody complex. The TdT-mediated dUTP nick end labeling (TUNEL) assay kit (40307ES20, YEASEN) was used to detect the apoptosis of cells in the tissue, and fluorescence-positive cells were counted by Image J. Five equivalent sections from each group were randomly selected, and six visual fields from each section were observed for statistical analysis.

2.11. Transcriptome sequencing

Eukaryotic transcriptome sequencing was performed on the bFGF group and the CFBP-bFGF group to reveal the molecular mechanism of CFBP-bFGF therapy in MI rats. Samples were collected at 5 days after continuous injections of the drug for 4w (about 33 days after MI) and sequenced by Sangon Biotech. Finally, the differential gene expression map was constructed using the bioinformatics method.

2.12. Fluorogenic quantitative PCR

TransZol Up Plus RNA Kit (ER501-01-V2, Transgen) was used to extract RNA ($n = 3$). The EasyScript® One-Step gDNA Removal and

cDNA Synthesis SuperMix kit (AE311-02, Transgen) was then used to reverse transcription and remove excess gDNA. 20 μL reaction system was selected using PerfectStart® Green qPCR SuperMix kit (AQ601-01-V2, Transgen), and gene primers of GAPDH, Vegfa, Fgf2, Hif1a, Mef2a, Tgfb1, Col1a1, Col3a1, Nppa, Caspase3, Bcl2 (Supplementary Table 1). Were added, respectively. The CFX96 Touch fluorescent quantitative PCR (Bio-rad) instrument was then used to perform the reaction according to the procedure provided by the kit. The primer was synthesized by Sangon Biotech.

2.13. Statistical analysis

The statistical analysis in this study was meticulously conducted using GraphPad Prism version 8.0.1 software (GraphPad Software, Inc., La Jolla). To compare data between two distinct groups, a Student's t-test was employed. In cases where multiple groups were analyzed, a one-way Analysis of Variance (ANOVA) was utilized, followed by a Tukey post hoc test to discern significant differences among the groups further. Statistical significance was rigorously defined as a p-value less than 0.05. To ensure clarity and consistency, all data were presented in the form of mean ± standard deviation (SD), with values rounded to two decimal places.

3. Results

3.1. Preparation and performance of recombinant CFBP-bFGF

Firstly, the native bFGF and CFBP-bFGF were purified and detected using SDS-PAGE and Western blot (Fig. 1A–B). Secondly, the bioactivity of bFGF and CFBP-bFGF was evaluated by promoting the proliferation of HSFs *in vitro*. As shown in Fig. 1C, the proliferative curve of bFGF and CFBP-bFGF was similar, indicating the fusion of CFBP peptide didn't impact the bioactivity of bFGF. Moreover, the effects of CFBP-bFGF on cardiomyocytes were also investigated. Under normal culture conditions, CFBP-bFGF and bFGF had similar impacts on H9c2 cardiomyocyte proliferation (Fig. 1D). Previous studies had reported that bFGF could protect cardiomyocytes against hypoxic injury [5]. Then, the protective effects of bFGF and CFBP-bFGF on the survival of H9c2 cells were explored in an OGD/R model. The results showed that CFBP-bFGF exhibited a significant protective effect at doses of 6.25 nM and 12.5 nM (Fig. 1E). That was due to CTGF being upregulated after hypoxia injury of H9c2 cells in a previous study, and this result was validated in Supplementary Fig. 2A. In addition, due to bFGF being an important angiogenic growth factor, then *in vitro* tubule formation assay was performed. As shown in Fig. 1F and G and Supplementary Fig. 2B, there were more tubular structures formed in the CFBP-bFGF group (55.17 ± 7.08) with significant differences compared with the PBS group (2.83 ± 5.98) and bFGF group (44.83 ± 5.04); tube forming branches of CFBP-bFGF group (154.00 ± 6.54) were also statistical more than PBS group (123.80 ± 9.09) and bFGF group (133.80 ± 15.92), and there was also significant difference between the bFGF group and PBS group. These results above suggested that the recombinant CFBP-bFGF had similar biological activity of bFGF with bFGF but had better protective effects on H9c2 cells in an OGD/R model *in vitro*.

3.2. CFBP-bFGF homed to the ischemic myocardium

Our previous studies demonstrated that CFBP-bFGF could target the microenvironment with highly expressed CTGF. Due to CTGF being revealed to upregulate after MI gradually, the expression of

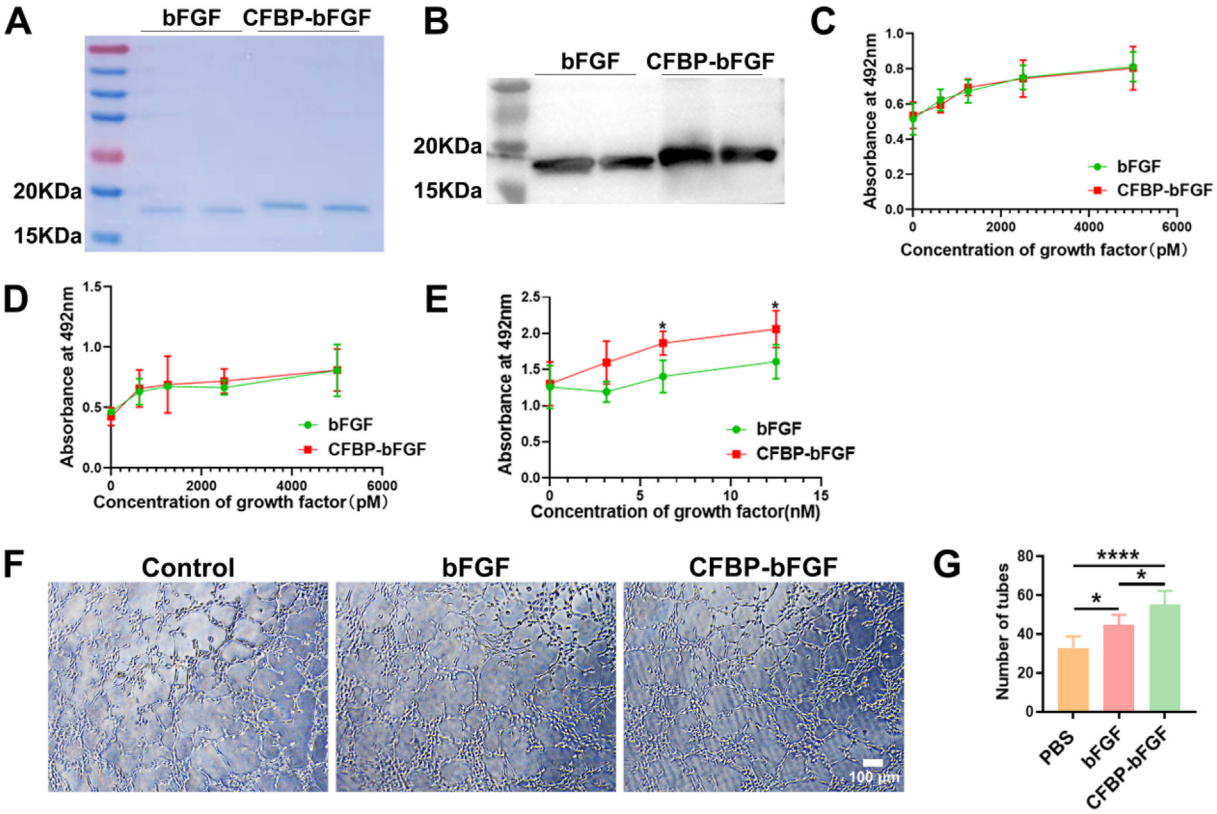

Fig. 1. Preparation and properties of CFBP-bFGF. (A) SDS-PAGE of purified bFGF and CFBP-bFGF; (B) Western blot of purified bFGF and CFBP-bFGF; (C) The biological activity assay of bFGF and CFBP-bFGF on HSF_S cells proliferation, n = 5; (D) The biological assay of bFGF and CFBP-bFGF on H9c2 cells proliferation, n = 5; (E) Cardiomyocytes protection assay on OGD/R model of H9c2 cells, n = 5; (F) Tube formation assay *in vitro*, n = 5; (G) Statistics of the number of tubules formed *in vitro*. Scale bar = 100 μm. Data were expressed as the mean ± SD. *$P < 0.05$, **$P < 0.01$, ***$P < 0.001$, ****$P < 0.0001$.

CTGF in the ischemic myocardium was assessed. The Western blot results showed that CTGF arose at 1 day following MI and exhibited a progressive increase until 2 weeks(Fig. 2A), suggesting that CTGF was a reliable target for the delivery of growth factors in MI, especially in a later stage. Therefore, the targeting capability of CFBP-bFGF by intravenous injection was detected at 3d, 1w, and 2w after MI. Quantitative ELISA assay revealed that in ischemic myocardium, the bFGF content in CFBP-bFGF group was 0.39 ± 0.02 μg/g at 3d after MI, 1.37 ± 0.03 μg/g at 1w after MI and 1.36 ± 0.07 μg/g at 2w after MI, which was notably higher compared to that of the bFGF group (0.34 ± 0.03 μg/g, 0.66 ± 0.06 μg/g, 1.01 ± 0.03 μg/g) respectively. Additionally, the serum bFGF content in bFGF group (2.52 ± 0.27 μg/mL, 2.13 ± 0.30 μg/mL, 3.04 ± 0.86 μg/mL) was observed to be higher than that in CFBP-bFGF group (2.33 ± 0.47 μg/mL, 1.87 ± 0.23 μg/mL, 2.33 ± 0.67 μg/mL), but with no statistical significance(Fig. 2B). These results were confirmed by Western blot, that the expression of bFGF in the ischemic myocardium of the CFBP-bFGF group was significantly higher than that in other groups at 3d, 1w, and 2w after MI(Fig. 1C and D). Therefore, these results suggested that CFBP-bFGF could target and retain in the ischemic heart effectively when administered intravenously.

3.3. CFBP-bFGF specifically bound to upregulated CTGF in ischemic hearts

To confirm whether CFBP-bFGF targeted delivered into the ischemic heart through interacting with the upregulated CTGF following MI, immunofluorescence staining of CTGF and bFGF was performed to investigate their potential co-localization. At 1w or 2w after MI, immunofluorescence staining revealed that the fluorescence intensity of CTGF was similar in all three groups, but the fluorescence intensity of bFGF was notably higher in the CFBP-bFGF group compared to both bFGF group and PBS group (Fig. 3A–E), which was consistent with the results obtained from ELISA and Western blot above. In addition, co-localization of bFGF and CTGF was more evident in the CFBP-bFGF group than in the other two groups, as shown in Fig. 3B–D and F–H. These results indicated that CFBP-bFGF was retained in the ischemic heart by specifically targeting CTGF.

3.4. CFBP-bFGF improved the recovery of cardiac function in MI rats

As the bioactivity and targeting capacity of CFBP-bFGF were validated, the regenerative effect of CFBP-bFGF for MI was further investigated. After MI, the recombinant proteins were repeated and administrated at 3d, 1w, 2w, 3w, and 4w after MI intravenously, and then the cardiac function was evaluated by Echocardiography at both 4w and 8w after MI. The echocardiographic results were shown in Table 1. Left ventricular ejection fraction (EF) and shortened fraction (FS) were the main indexes to evaluate cardiac function. The results revealed that EF and FS in the CFBP-bFGF group (85.01 ± 4.04 %, 42.77 ± 4.17 %) were significantly increased compared with those in PBS group (48.09 ± 4.65 %, 22.10 ± 3.78 %) and bFGF group (73.43 ± 3.42 %, 32.96 ± 4.18 %) at 4 weeks after administration, and they had statistical difference between bFGF and PBS group (Table 1). Other indicators such as LVDd (mm), LVDs (mm), LVPWd (mm) of CFBP-bFGF and bFGF group also had significant differences compared with the PBS group, but there was no difference between CFBP-bFGF and bFGF group; and the IVSs (mm) of CFBP-bFGF had measurable difference with bFGF and PBS group, but there was no significant difference between bFGF group and PBS group. Similar results were also observed at 8 weeks (Table 1), that the major indicator of cardiac function in the CFBP-bFGF group was better than those in the bFGF group and PBS group. Therefore, these results indicated that CFBP-bFGF could promote cardiac function recovery in rats with MI.

3.5. CFBP-bFGF attenuated morphological injury and ventricular remodeling

Consistent with cardiac function evaluation, the H&E staining was used for the histological evaluation. As shown in Fig. 4A and B, the histological structure of the PBS group showed extensive cardiomyocyte loss and interstitial fibrosis, but in the bFGF group, especially in the CFBP-bFGF group, the myocardial injury and fibrosis were alleviated with well arranged myocardial fibres. Therefore, these results indicated that CFBP-bFGF could alleviate the histological injury. It has been reported following MI, the infarcted hearts underwent the cardiomyocyte loss and interstitial fibrosis, which would result in ventricular remodeling and scar

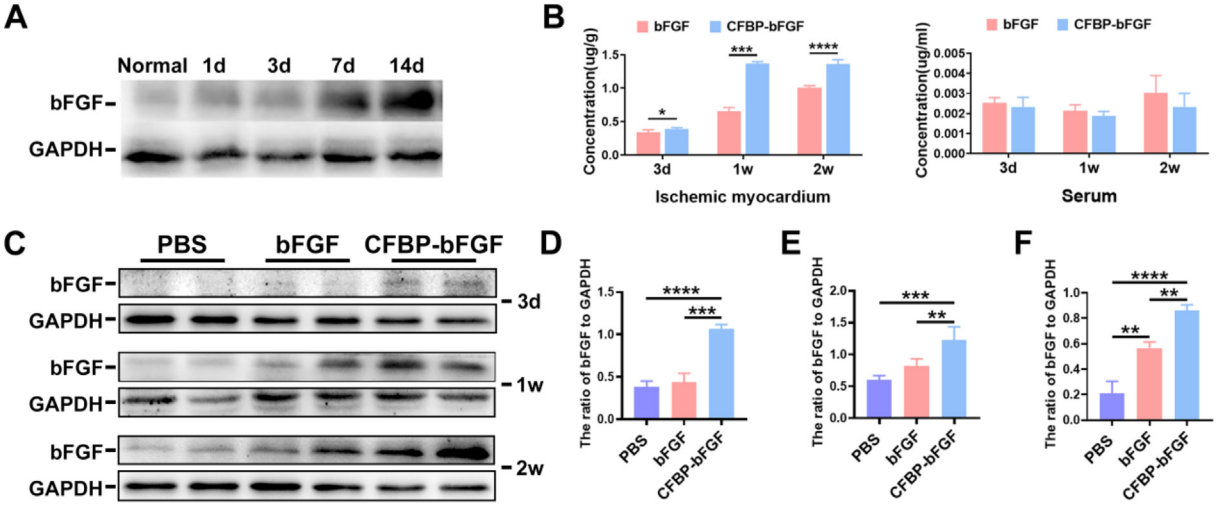

Fig. 2. Evaluation of the targeting efficiency of CFBP-bFGF in ischemic myocardium. (A) Western blot analysis of CTGF expression in ischemic myocardium at 1d, 3d, 1w and 2w after MI; (B)The content of bFGF in ischemic myocardium and serum was determined by ELISA at 3d, 1w and 2w after MI; (C) Western blot analysis of bFGF in ischemic myocardium at 3d, 1w and 2w after MI; (D) The statistical analysis of Western blot statistical analysis of bFGF at 3d after MI; (E) The statistical analysis of Western blot statistical analysis of bFGF at 1w after MI; (F) The statistical analysis of Western blot statistical analysis of bFGF at 2w after MI. Data were expressed as the mean ± SD. *$P < 0.05$, **$P < 0.01$, ***$P < 0.001$, ****$P < 0.0001$, n = 5.

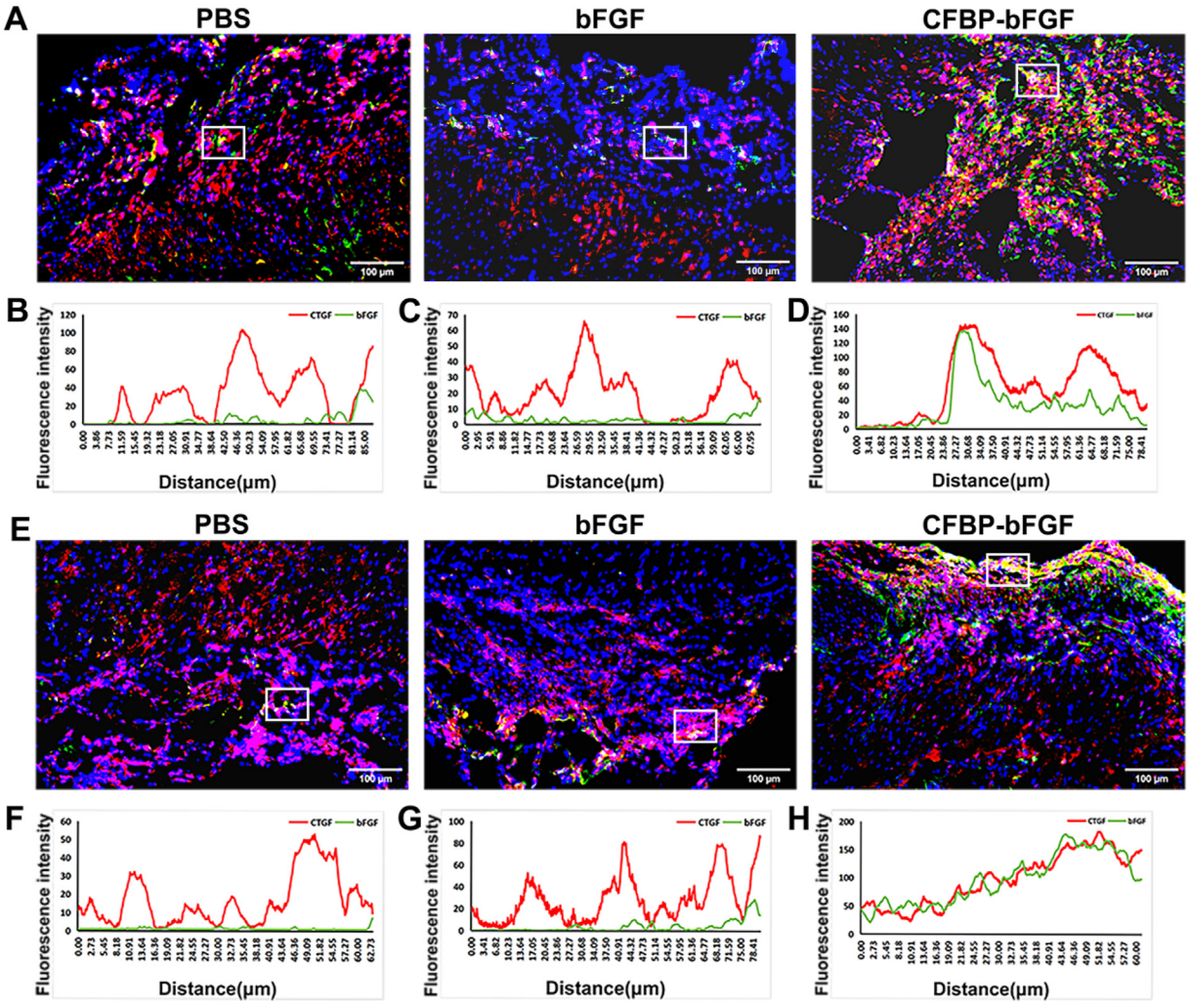

Fig. 3. Colocalization of CFBP-bFGF and CTGF in ischemic myocardial tissue. (A) Immunofluorescence staining of CTGF (red) and bFGF (green) in ischemic myocardium at 1w after MI. Yellow staining indicates colocalization; (B)The colocalization analysis of CTGF and bFGF in PBS group; (C) The colocalization analysis of CTGF and bFGF in bFGF group; (D) The colocalization analysis of CTGF and bFGF in CFBP-bFGF group; (E) Immunofluorescence staining of CTGF (red) and bFGF (green) in ischemic myocardium 2w after MI. Yellow staining indicates colocalization; (F) The colocalization analysis of CTGF and bFGF in the PBS group; (G) The colocalization analysis of CTGF and bFGF in the bFGF group; (H) The colocalization analysis of CTGF and bFGF in CFBP-bFGF group. Scale bar = 100 μm, n = 3.

Table 1
Results of echocardiographic parameters 4 weeks and 8 weeks after MI.

		EF(%)	FS(%)	LVDd(mm)	LVDs(mm)	IVSs(mm)	LVPWd(mm)
4w	PBS Group	48.09 ± 4.65	22.10 ± 3.78	12.11 ± 0.98	9.87 ± 1.34	2.10 ± 0.50	2.35 ± 0.53
	bFGF Group	73.43 ± 3.42**	32.96 ± 4.18**	7.50 ± 0.96**	4.27 ± 0.58**	2.46 ± 0.43	4.69 ± 0.68**
	CFBP-bFGF Group	85.01 ± 4.04**/##	42.77 ± 4.17**/##	6.70 ± 0.75**	3.10 ± 0.52**	3.18 ± 0.19**/#	4.45 ± 0.80**
8w	PBS Group	46.67 ± 1.65	26.04 ± 3.50	10.04 ± 0.58	7.52 ± 0.64	2.42 ± 0.28	2.35 ± 0.30
	bFGF Group	54.36 ± 3.66*	35.52 ± 5.25**	7.63 ± 0.50**	5.28 ± 0.89**	2.81 ± 0.38*	2.77 ± 0.39
	CFBP-bFGF Group	78.50 ± 5.62**/##	54.73 ± 5.35**/##	6.70 ± 0.87**	4.05 ± 0.62**	3.20 ± 0.45**/#	3.50 ± 0.51**/##

EF(%), ejection fraction; FS(%), indicates fractional shortening; LVDs (mm), left ventricular systolic diameter; LVDd (mm), left ventricular end-diastolic diameter; IVSs (mm), inter-ventricular septum end-stolic thickness; LVPWd (mm), left ventricular posterior wall thickness. Data are mean ± SD; *: CFBP-bFGF VS PBS or bFGF VS PBS, #: CFBP-bFGF VS bFGF; $^{*}P < 0.05$, $^{**}P < 0.01$; $^{\#}P < 0.05$, $^{\#\#}P < 0.01$, n = 6.

formation [13]. Subsequently, the ventricular remodeling was further investigated. As shown in Fig. 4C–F, Masson staining showed infarct size was 21.03 ± 2.94 %, 29.90 ± 5.76 %, 37.47 ± 5.41 % in CFBP-bFGF group, bFGF group, and PBS group respectively, and there was a significant difference between CFBP-bFGF group and PBS group. Furthermore, the statistical analysis of wall thickness revealed the thickness of the CFBP-bFGF group was 4.16 ± 0.12 mm, which was markedly greater than that of the bFGF group (2.32 ± 0.34 mm) and PBS group (2.12 ± 0.37 mm). These results suggested CFBP-bFGF could attenuate morphological injury and ventricular remodeling caused by hypoxia injury.

3.6. CFBP-bFGF promoted angiogenesis and protected cardiomyocyte survival in the infarcted hearts

As bFGF was an essential regulator of angiogenesis and cardiomyocyte protection, then vascularization, and cardiomyocyte survival were detected by immunostaining. To identify arterioles

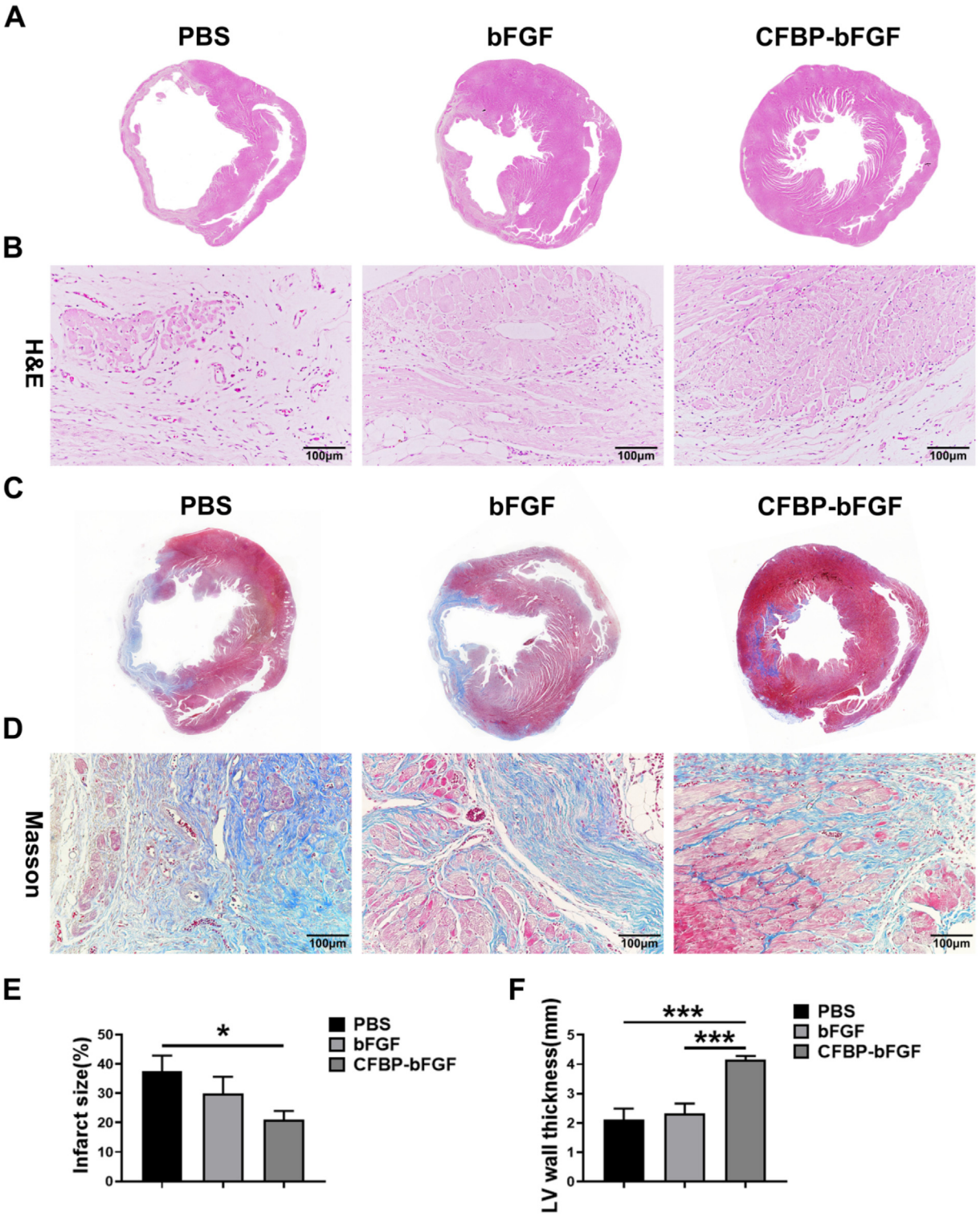

Fig. 4. The evaluation of cardiac function after CFBP-bFGF or bFGF intravenous administration. (A) H&E staining panoramic scan representation of each group; (B) H&E staining of myocardial infarction; (C) Masson staining panoramic scan representation of each group; (D) Masson staining of infarcted myocardium; (E) Statistical analysis of infarct size; (F) Statistical analysis of LV wall thickness. Data represent mean ± SD, $*P < 0.05$, $**P < 0.01$, $***P < 0.001$, n = 5.

with a visible lumen, Anti-α-SMA immunostaining was employed, while Anti-vWF immunostaining was utilized to detect the distribution of capillaries. As shown in Fig. 5A and B, the number of arterioles labeled with α-SMA in the CFBP-bFGF group was 20.44 ± 1.42, which was superiorly higher compared to both the bFGF group (14.67 ± 1.32) and PBS group (13.22 ± 0.83). Subsequently, the number of capillaries positive for immunostaining in the infarcted area was also significantly greater in the CFBP-bFGF group (75.67 ± 2.08) compared to both the bFGF group (59.00 ± 8.54) and PBS group (36.00 ± 4.36), and there was a significant difference between bFGF group and PBS group (Fig. 5A–C). To evaluate whether CFBP-bFGF protected cardiomyocytes in the

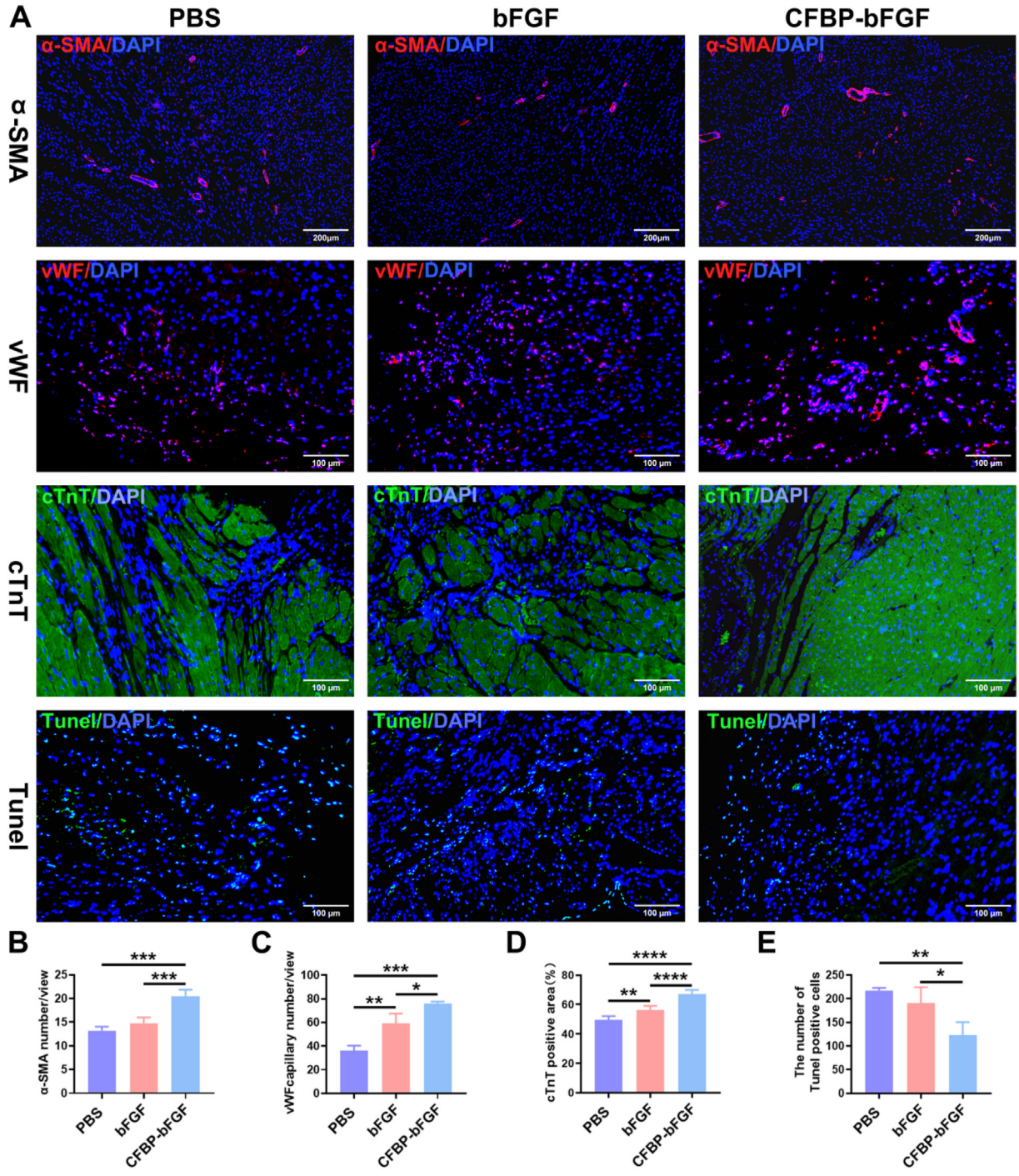

Fig. 5. Evaluation of blood vessel regeneration, cardiocyte survival, and apoptosis after CFBP-bFGF or bFGF by intravenous administration. (A) Immunofluorescence staining of α-SMA, vWF, cTnT, and Tunel staining in ischemic myocardium; (B) Statistical analysis of the number of arterioles labeled by α-SMA; (C) Statistical analysis of the number of capillaries labeled by vWF; (D) Statistical analysis of the positive area of myocardium labeled by cTnT; (E) Statistical analysis of the number of TUNEL-positive cells. Scale bar = 100 μm. Data were expressed as the mean ± SD. *$P < 0.05$, **$P < 0.01$, ***$P < 0.001$, ****$P < 0.0001$, n = 6.

infarcted area, Anti-cTnT antibody was used to identify cardiomyocytes, the results showed cTnT-positive area of CFBP-bFGF group (67.17 ± 2.78 %) were more than those in bFGF group (56.08 ± 3.05 %) and PBS group (49.48 ± 2.69 %), and also there was statistical difference of positive area between bFGF group and PBS group (Fig. 5A–D). In addition, the cardiomyocytes' survival was also verified by TUNEL staining, which detected the cell apoptosis in the ischemic heart. Notably, the CFBP-bFGF group (122.30 ± 28.29) and the bFGF group (191.00 ± 33.42) exhibited a significantly lower number of apoptotic cells compared to the PBS group (217.30 ± 5.69) (Fig. 5A–E). These results demonstrated that CFBP-bFGF effectively enhanced angiogenesis and protected cardiomyocytes in the infarcted heart. This beneficial effect was attributed to the homing capacity of CFBP-bFGF towards ischemic myocardium, enabling targeted enrichment of bFGF and subsequent therapeutic action in the infarction zone.

3.7. Potential molecular mechanism of CFBP-bFGF in the therapy of MI

Finally, Transcriptome analysis was used to analyze the molecular mechanism between CFBP-bFGF and bFGF in the process of MI repair. As shown in Fig. 6A, gene ontology (GO) analysis showed that significantly enriched GO items in the biological processes (BP) category included signal transduction regulation, vascular development, angiogenesis, inflammatory response, and cell response to transforming growth factor β stimulation. In the cell components (CC) category, cytoskeleton, extracellular matrix, and myofibrillar gene products showed significant enrichment. In the molecular function (MF) category, growth factor activity, signal transducer activity et al. were enriched. The KEGG database was used to determine the signaling pathways involved in cardiac repair. As shown in Fig. 6B, compared with the bFGF group, the MAPK signaling pathway, AMPK signaling pathway, and JAK-STAT signaling pathway were significantly activated in the CFBP-bFGF group compared with the bFGF group; on the other hand, Chemokine signaling pathway, IL-17 signaling pathway, and TGF-β signaling pathway were significantly downregulated. Differential expression gene (DEG) analysis showed that compared with the bFGF group, 94 genes were up-regulated, and 105 genes were down-regulated in the CFBP-bFGF group (Fig. 6C). Differential expression genes (DEGs) were identified by analyzing FPKM data (Fig. 6D). The results showed that compared with the bFGF group, a series of genes such

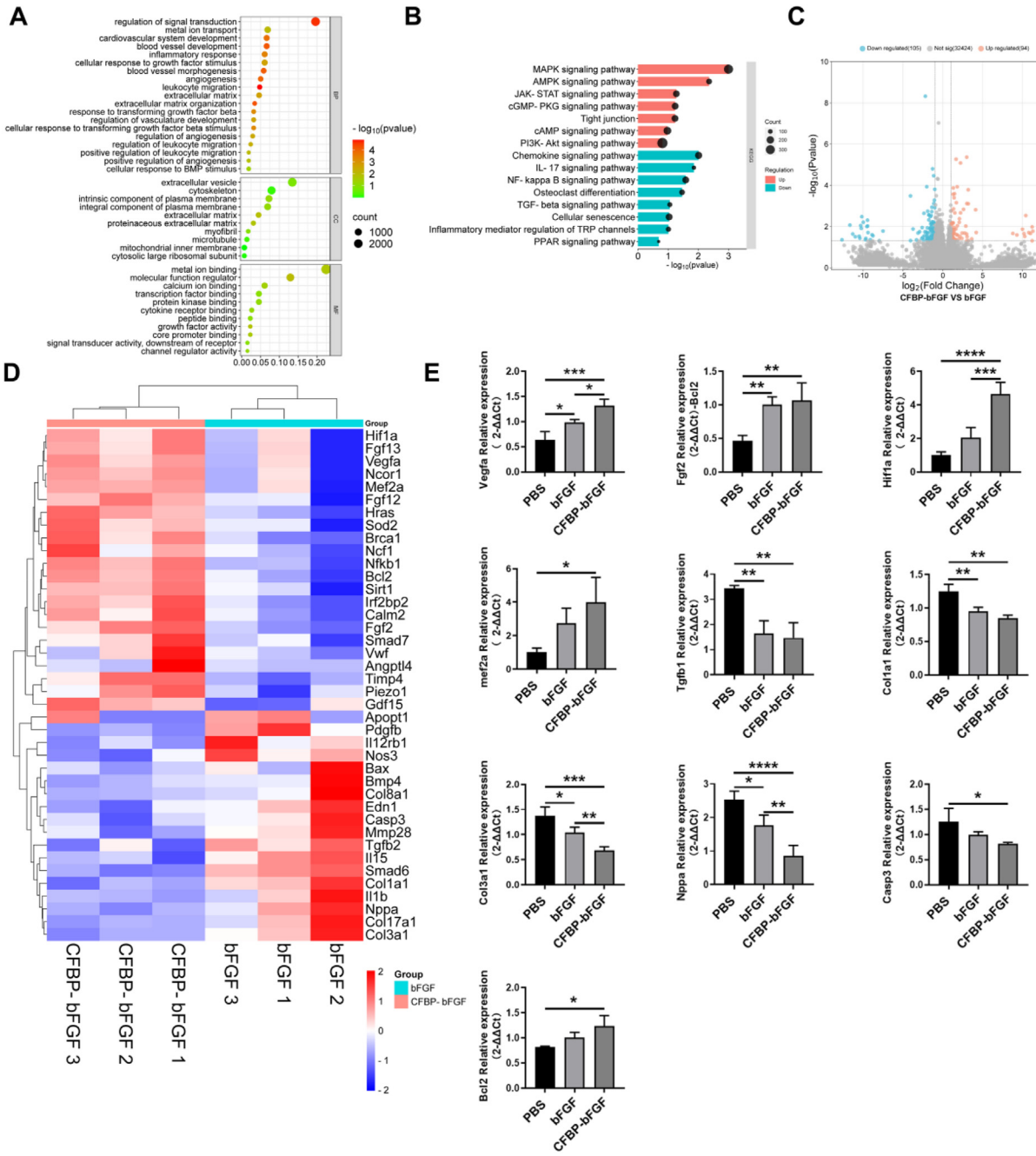

Fig. 6. Transcriptome analysis to determine the mechanism of CFBP-bFGF mediated ischemic myocardial repair. (A) Gene ontology (GO) analysis after continuous injection for one month; (B) KEGG analysis; (C)Differential gene expression in the bFGF group and CFBP-bFGF group; (D) Significantly different gene profiles associated with ischemic myocardial regeneration and repair, n = 3; (E) qPCR validation of mRNA expression trends of key genes, *$P < 0.05$, **$P < 0.01$, ***$P < 0.001$, ****$P < 0.0001$, n = 3.

as pro-angiogenic genes such as *Vegfa*, *Fgf2*, *Fgf13*, cardiomyocytes repair related gene-hypoxia inducible factor-1α (*Hif1a*), Myocyte Specific Enhancer Factor 2a (*Mef2a*) were significantly upregulated; on the contrary, fibrosis-related genes-Transforming growth factor β (*Tgfβ*), Smad homology 6 (*Smad6*) and collagen a1 (*Col1a1*) was downregulated. These key genes involved in the Transcriptome analysis were validated by the qPCR, as shown in Fig. 6E.

3.8. CFBP-bFGF alleviated cardiac fibrosis through the TGF-β signaling pathway

As CFBP-bFGF was shown to inhibit fibrosis-related signaling pathways and genes by Transcriptome analysis, the cardiac fibrosis was further confirmed by Anti-Collagen and Anti-Vemintin immunostaining. As shown in Fig. 7A and B, the immunofluorescent intensity of Collagen I and Vimentin in ischemic myocardium was markedly decreased in the CFBP-bFGF and PBS group, and there was also a significant difference in Vimentin expression between the bFGF group and the CFBP-bFGF group. Furthermore, the expression of the TGF-β signaling pathway was detected. As shown in Fig. 7C, TGF-β1 and its key downstream effector Smad3, as well as *p*-Smad3 was significantly decreased in the CFBP-bFGF group compared with the bFGF group and PBS group. Still, the expression of Smad7 was upregulated, which was consistent with its gene expression. Therefore, these results indicated CFBP-bFGF could alleviate ventricular remodeling and cardiac fibrosis through TGF-β signaling.

4. Discussion

In recent years, MI has revealed a trend of youthfulness and high incidence, which has increased significantly [14]. The treatment of myocardial infarction focuses on restoring blood flow to the coronary arteries and reducing myocardial damage as soon as possible [15]. In the regenerative therapy of MI, the targeted delivery of growth factors has emerged as a promising strategy [16].

bFGF is a crucial growth factor that exhibits a diverse range of biological functions, including the stimulation of angiogenesis, acceleration of wound healing and repair processes, as well as the promotion of tissue regeneration [17]. In the therapy of MI, bFGF was revealed to facilitate cardiac repair in a series of animal MI models. Alternative targeting delivery strategies were investigated to increase its regional concentration. bFGF was demonstrated to encapsulate in Polycaprolactone (PCL), poly(lactide-*co*-glycolide) (PLGA), acetalated dextran(AcDex) microparticles for sustained release, which promoted angiogenesis and cardiac regeneration [4,18,19]; it could also be incorporated in gelatin hydrogels, chitosan hydrogels to improve ventricular function through angiogenesis and cardiac protection [20–22]. In recent years, a responsive-release delivery system was developed. For example, acoustically-responsive scaffolds were constructed for the controlled release of bFGF to achieve the spatially-directed angiogenesis [23,24], and a dual functional MI-responsive hydrogel formed with glutathione (GSH)-modified collagen hydrogel (collagen-GSH) and GST-TIMP-bFGF, which released bFGF responsive to upregulated matrix metalloproteinase-2/9 (MMP-2/9) in microenvironment after MI and promoted the recovery of MI rats [25]. In the present study, in order to realize repeated administration of bFGF, specifically in ischemic myocardium, recombinant CFBP-bFGF was designed to recognize upregulated CTGF in the injured microenvironment, guide and target release of bFGF into ischemic myocardium by intravenous administration.

Then, the biological activity, homing capacity, and therapeutic efficacy of CFBP-bFGF in MI were further evaluated. Firstly, *in vitro* cell proliferation assays showed that bFGF and CFBP-bFGF both efficiently promoted the growth of HSF cells and H9c2 cells in normal conditions (Fig. 1C and D), but had a significant protective

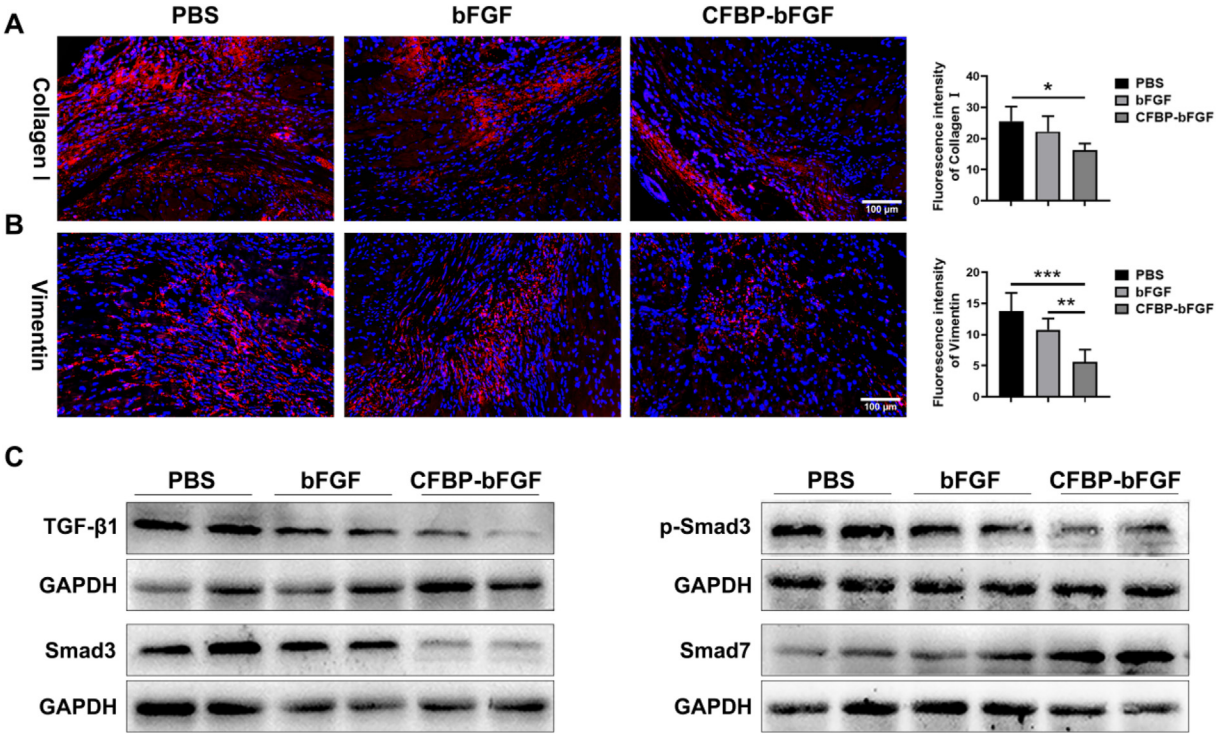

Fig. 7. The administration of CFBP-bFGF can alleviate MI-induced cardiac fibrosis and alleviate adverse cardiac remodeling. (A) Immunofluorescence staining and statistical analysis of collagenI; (B) Immunofluorescence staining and statistical analysis of Vimentin; (C)Western blot results of TGF-β pathway and Smad7, *$P < 0.05$, **$P < 0.01$, ***$P < 0.001$, n = 6.

effect on hypoxic H9c2 (Fig. 1E). That might be due to CTGF being an important regulator after ischemic injury *in vitro* or *in vivo*, and the tendency of CTGF in (the OGD/R) model of H9c2 cells was confirmed in Supplementary Fig. 1B, which was upregulated compared with normal conditions. Due to the CFBP-bFGF targeting upregulated CTGF in hypoxic H9c2 cells, it played an enhanced cardioprotective effect compared with bFGF. Additionally, as bFGF was an angiogenic factor, the *in vitro* tube formation assay was also performed. Both bFGF and CFBP-bFGF showed notably more tube formation compared to the control group, and CFBP-bFGF also showed a stronger angiogenic effect compared to the bFGF group (Fig. 1F and G). Previous studies have reported that CTGF participated in blood vessel formation in tumors and age-related vascular diseases [26,27]. Direct evidence showed that the secretion of CTGF increased from growth factors that treated HUVECs, which improved the migration and network formation of HUVECs [28,29]. Correlated with increased CTGF, CFBP-bFGF promoted the number of tube formations *in vitro*. These results indicated that in normal conditions, CFBP-bFGF had a similar biological activity with native bFGF, while it also could interact with upregulated CTGF in the microenvironment to enhance the protective or angiogenic effect of bFGF due to prolonged release.

The homing capacity of CFBP-bFGF *in vivo* was further investigated. Due to CTGF gradually upregulating after MI, we detected the targeting efficiency of CFBP-bFGF at different times of MI by intravenous administration. That would help to determine the time and frequency of CFBP-bFGF administration. Quantitative ELISA assay and Western blot revealed the amount of CFBP-bFGF in the ischemic myocardium was statistically higher than that in the bFGF group at 3d, 1w, and 2w after MI (Fig. 2B–D). And most CFBP-bFGF was observed to be co-localization with upregulated CTGF in ischemic myocardium (Fig. 3A–H). As a result, CFBP-bFGF was administrated through the tail vein at 3d, 1w, 2w, 3w, and 4w after MI to evaluate its therapeutic effects in the following animal experiments. At 4w and 8w after MI, the cardiac function was detected by Echocardiography. The results showed the administration of CFBP-bFGF significantly improved the cardiac recovery of MI rats, and the echocardiographic indicators such as EF and FS had statistical differences between the CFBP-bFGF group and the bFGF group (Table 1). In accordance with functional recovery, the histological evaluation revealed CFBP-bFGF could alleviate ventricular remodeling, promote blood vessel regeneration, protect cardiomyocyte survival, and prevent cardiomyocyte apoptosis (Figs. 4 and 5), indicating CFBP-bFGF was beneficial for cardiac repair that improved both morphological and functional recovery after MI.

Finally, the molecular mechanism of CFBP-bFGF in the repair of ischemic myocardium was still unknown. In our study, transcriptome analysis uncovered that a series of signaling pathways and a population of genes were upregulated or downregulated in the CFBP-bFGF group compared with the bFGF group (Fig. 6B–D). Compared with the bFGF group, MAPK signaling pathway, AMPK signaling pathway, and JAK-STAT signaling pathway were significantly activated in CFBP-bFGF group, while Chemokine signaling pathway, IL-17 signaling pathway and TGF-β signaling pathway were significantly downregulated in the CFBP-bFGF group. Consistent with previous studies, differential expression genes results revealed angiogenesis-related genes, cardiomyocyte protection-related gene was upregulated, and fibrosis-related genes, and apoptosis-related genes were downregulated. These alterations of genes were correlated with the biological effects of bFGF, which was verified by qPCR in Fig. 6D. In addition, the antifibrosis effect of CFBP-bFGF was further investigated due to the evidently decreased gene expression of *Tgfb1, Col1a1*. Under ischemic conditions, fibroblasts were activated and transformed into myofibroblasts, secreting abundant collagens. It has been shown that the reduction of myofibroblasts by targeting TGF-β signaling to inhibit fibroblast activation reduced collagen synthesis [30]. Then, immunostaining of Collagen I and Vimentin was performed. And the results of Fig. 7 showed the expression of Collagen I and Vimentin was evidently attenuated in the CFBP-bFGF group, which indicated the role of CFBP-bFGF in the regulation of endothelial-to-mesenchymal transition and subsequent collagen deposition. This process was mediated by TGF-β/Smad 3 signaling pathway (Fig. 7A–C).

Besides the prolonged release of bFGF in ischemic myocardium, we were also interested in the potential function of CFBP peptide. The interacting protein of CFBP peptide-CTGF was a common key regulator for tissue fibrosis, which was a cysteine-rich matricellular protein involved in the control of multiple biological and pathological processes [31]. In the heart, CTGF was strongly produced by injured cardiomyocytes, subsequently activating the fibroblasts and contributing to myofibroblast differentiation and persistence [31]. Furthermore, CTGF inhibition by its specific monoclonal antibody (CTGF mAb) during MI repair was demonstrated to improve survival, attenuate LV dysfunction, and reduce post-MI LV hypertrophy and fibrosis [32]. The question of whether the interaction of CFBP peptide and CTGF would influence the bioactivity of CTGF was unknown. It was reported that CTGF consisted of four essential domains, including IGFBP (Gln27-Lys98), VWC(Ala101-Asp167), TSP1 (Asn198-Glu243) and CT (Cys256-Pro330) from N-terminal to C-terminal. And each domain could specifically bind with different proteins and thereby play different functions [33]. Therefore, the binding of CFBP peptide and CTGF was imitated and analyzed by Wemol (Supplementary Fig. 2). The CFBP peptide was predicted to bind with the spatial structural domain formed by Pro51, Gly62, Leu75, and Trp171, which were mainly located in the IGFBP and VWC domains. It was observed that the IGFBP domain was in charge of the combination of CTGF and insulin-like growth factor (IGF), which was involved in the process of matrix accumulation, and the VWC domain was the region that CTGF bonded to BMPs or TGF-β, which served as an antagonist of BMPs or chaperone to enhance TGF-β signaling function conversely [34]. These results suggested that CFBP peptide might competitively bind CTGF with IGF or TGF-β, which would decrease tissue fibrosis and matrix deposition. In the future, the interaction of CFBP-bFGF and CTGF will be further explored *in vitro* and *in vivo*, including the influence on downstream signaling pathways and subsequent biological processes.

Currently, controlled and sustained growth factor release systems had been extensively studied to improve the therapeutic effects of the proteins. Besides the growth factor encapsulation into biomaterial scaffolds, the functional modification of growth factor by gene engineering was another alternative strategy. In present study, the specific peptide CFBP was fused with bFGF to construct CFBP-bFGF, the recombinant CFBP-bFGF could recognize the CTGF in injured myocardium and realize the targeting delivery of bFGF with proper dosage and excellent spatiotemporal specificity. In addition, the bioinformatics and its subsequent experimental analysis revealed the interaction of CFBP peptide and CTGF would impact the pro-fibrotic effect of CTGF. These results indicated the CFBP-bFGF would be a bio-functional growth factor, that promoted the cardiac repair and decreased the cardiac fibrosis. These were the advantages of present studies. However, the optimal dosage, injection time and frequency of CFBP-bFGF for the therapy of MI was still unknown and the potential molecular mechanisms of CFBP-bFGF was also unclear. These were the limitations of present studies. Further studies in large animal models and the potential molecular mechanisms of CFBP-bFGF will be explored to provide evidence for the application of clinical MI therapy.

In conclusion, a recombinant CFBP-bFGF was constructed, which could target deliver bFGF in response to upregulated CTGF in ischemic myocardium by intravenous administration. The CFBP-bFGF was revealed to promote angiogenesis, protect cardiomyocytes, and prevent cell apoptosis, which finally improved the functional recovery in rats with MI. In addition, the further transcriptome analysis displayed CFBP-bFGF inhibited the fibrosis-related signaling pathway and genes compared to bFGF, which directly attenuated cardiac remodeling and fibrosis. Through the targeting delivery, CFBP-bFGF could realize repeated intravenous administration of bFGF in low dosage but with high efficiency, and provide a potential therapeutic strategy for MI.

Authorship contribution statement

Shuwei Sun contributed to the study conception, design and the original draft; Fengzheng Zhu and Qingling Xu contributed to methodology and the original draft; Xianglin Hou and Weihong Nie provided data curation; Kaiyan Su provided analysis, visualization, and validation; Li Wang and Zhuo Liu performed and discussed the results with data analysis; Tao Shan performed conceptualization and project administration; Chunying Shi provided funding and supervised the project. All authors read and approved the final article.

Consent for publication

The authors declare no competing financial interest.

Funding

This work was supported by the Natural Science Foundation of Shandong Province (ZR2023MC168), and the Key R&D Program of Shandong Province (2019GSF107037).

Declaration of competing interest

The authors declare that they have no competing interests.

Acknowledgement

We thank Qingdao University Instrument sharing platform for its technical help; Thanks to Lulu Song of Laboratory Animal Center of Qingdao University for her technical help in animal echocardiography measurement.

Data and materials availability

All data required of the paper are included in the paper and/or the Supplementary Materials. The other related data may be requested from the authors.

Appendix A. Supplementary data

Supplementary data to this article can be found online at https://doi.org/10.1016/j.reth.2025.01.006.

References

[1] Martin SS, Aday AW, Almarzooq ZI, Anderson CAM, Arora P, Avery CL, et al. 2024 heart disease and stroke Statistics: a report of us and global data from the American heart association. Circulation 2024;149(8):e347–913.
[2] Sutton MG, Sharpe N. Left ventricular remodeling after myocardial infarction: pathophysiology and therapy. Circulation 2000;101(25):2981–8.
[3] Fan Z, Xu Z, Niu H, Sui Y, Li H, Ma J, et al. Spatiotemporal delivery of basic fibroblast growth factor to directly and simultaneously attenuate cardiac fibrosis and promote cardiac tissue vascularization following myocardial infarction. J Contr Release 2019;311:233–44.
[4] Arunkumar P, Dougherty JA, Weist J, Kumar N, Angelos MG, Powell HM, et al. Sustained release of basic fibroblast growth factor (bFGF) encapsulated Polycaprolactone (PCL) microspheres promote angiogenesis in vivo. Nanomaterials 2019;9(7).
[5] Tong G, Liang Y, Xue M, Chen X, Wang J, An N, et al. The protective role of bFGF in myocardial infarction and hypoxia cardiomyocytes by reducing oxidative stress via Nrf2. Biochem Biophys Res Commun 2020;527(1):15–21.
[6] Simons M, Annex BH, Laham RJ, Kleiman N, Henry T, Dauerman H, et al. Pharmacological treatment of coronary artery disease with recombinant fibroblast growth factor-2: double-blind, randomized, controlled clinical trial. Circulation 2002;105(7):788–93.
[7] Wang Y, Wang D, Wu C, Wang B, He S, Wang H, et al. MMP 9-instructed assembly of bFGF nanofibers in ischemic myocardium to promote heart repair. Theranostics 2022;12(17):7237–49.
[8] Song S, Hou X, Zhang W, Liu X, Wang W, Wang X, et al. Specific bFGF targeting of KIM-1 in ischemic kidneys protects against renal ischemia-reperfusion injury in rats. Regen Biomater 2022;9:rbac029.
[9] Nagase K, Nagaoka M, Nakano Y, Utoh R. bFGF-releasing biodegradable nanoparticles for effectively engrafting transplanted hepatocyte sheet. J Contr Release 2024;366:160–9.
[10] Yang Y, Shi C, Hou X, Zhao Y, Chen B, Tan B, et al. Modified VEGF targets the ischemic myocardium and promotes functional recovery after myocardial infarction. J Contr Release 2015;213:27–35.
[11] Mann AP, Scodeller P, Hussain S, Braun GB, Mölder T, Toome K, et al. Identification of a peptide recognizing cerebrovascular changes in mouse models of Alzheimer's disease. Nat Commun 2017;8(1):1403.
[12] Deng J, Zhang X, Yin M, Cao W, Zhang B, Liu Q, et al. Modified CFBP-bFGF targeting to ischemic brain promoted the functional recovery of cerebral ischemia. J Contr Release 2023;353:462–74.
[13] Tallquist MD. Cardiac fibroblast diversity. Annu Rev Physiol 2020;82:63–78.
[14] Diseases GBD, Injuries C. Global incidence, prevalence, years lived with disability (YLDs), disability-adjusted life-years (DALYs), and healthy life expectancy (HALE) for 371 diseases and injuries in 204 countries and territories and 811 subnational locations, 1990-2021: a systematic analysis for the Global Burden of Disease Study 2021. Lancet 2024;403(10440):2133–61.
[15] Cao W, Zhang H, Zhou N, Zhou R, Zhang X, Yin J, et al. Functional recovery of myocardial infarction by specific EBP-PR1P peptides bridging injectable cardiac extracellular matrix and vascular endothelial growth factor. J Biomed Mater Res 2023;111(7):995–1005.
[16] Braile M, Marcella S, Cristinziano L, Galdiero MR, Modestino L, Ferrara AL, et al. VEGF-A in cardiomyocytes and heart diseases. Int J Mol Sci 2020;21(15).
[17] Padua RR, Sethi R, Dhalla NS, Kardami E. Basic fibroblast growth factor is cardioprotective in ischemia-reperfusion injury. Mol Cell Biochem 1995;143(2):129–35.
[18] Suarez S, Grover GN, Braden RL, Christman KL, Almutairi A. Tunable protein release from acetalated dextran microparticles: a platform for delivery of protein therapeutics to the heart post-MI. Biomacromolecules 2013;14(11):3927–35.
[19] Nelson DM, Hashizume R, Yoshizumi T, Blakney AK, Ma Z, Wagner WR. Intramyocardial injection of a synthetic hydrogel with delivery of bFGF and IGF1 in a rat model of ischemic cardiomyopathy. Biomacromolecules 2014;15(1):1–11.
[20] Kumagai M, Minakata K, Masumoto H, Yamamoto M, Yonezawa A, Ikeda T, et al. A therapeutic angiogenesis of sustained release of basic fibroblast growth factor using biodegradable gelatin hydrogel sheets in a canine chronic myocardial infarction model. Heart Ves 2018;33(10):1251–7.
[21] Li Z, Masumoto H, Jo JI, Yamazaki K, Ikeda T, Tabata Y, et al. Sustained release of basic fibroblast growth factor using gelatin hydrogel improved left ventricular function through the alteration of collagen subtype in a rat chronic myocardial infarction model. Gen Thorac Cardiovasc Surg 2018;66(11):641–7.
[22] Fu B, Wang X, Chen Z, Jiang N, Guo Z, Zhang Y, et al. Improved myocardial performance in infarcted rat heart by injection of disulfide-cross-linked chitosan hydrogels loaded with basic fibroblast growth factor. J Mater Chem B 2022;10(4):656–65.
[23] Moncion A, Lin M, O'Neill EG, Franceschi RT, Kripfgans OD, Putnam AJ, et al. Controlled release of basic fibroblast growth factor for angiogenesis using acoustically-responsive scaffolds. Biomaterials 2017;140:26–36.
[24] Huang L, Quesada C, Aliabouzar M, Fowlkes JB, Franceschi RT, Liu Z, et al. Spatially-directed angiogenesis using ultrasound-controlled release of basic fibroblast growth factor from acoustically-responsive scaffolds. Acta Biomater 2021;129:73–83.
[25] Fan C, Shi J, Zhuang Y, Zhang L, Huang L, Yang W, et al. Myocardial-infarction-responsive smart hydrogels targeting matrix metalloproteinase for on-demand growth factor delivery. Adv Mater 2019;31(40):e190290.
[26] Shen YW, Zhou YD, Chen HZ, Luan X, Zhang WD. Targeting CTGF in cancer: an emerging therapeutic opportunity. Trends Cancer 2021;7(6):511–24.

[27] Ungvari Z, Valcarcel-Ares MN, Tarantini S, Yabluchanskiy A, Fülöp GA, Kiss T, et al. Connective tissue growth factor (CTGF) in age-related vascular pathologies. Geroscience 2017;39(5–6):491–8.
[28] Lee MS, Ghim J, Kim SJ, Yun YS, Yoo SA, Suh PG, et al. Functional interaction between CTGF and FPRL1 regulates VEGF-A-induced angiogenesis. Cell Signal 2015;27(7):1439–48.
[29] Shimo T, Shimatani M, Tanimura A, Takigawa M. Angiogenesis assays for the analysis of CCN proteins. Methods Mol Biol 2023;2582:295–308.
[30] Ceauşu Z, Socea B, Costache M, Predescu D, Şerban D, Smarandache CG, et al. Fibroblast involvement in cardiac remodeling and repair under ischemic conditions. Exp Ther Med 2021;21(3):269.
[31] Gu C, Shi X, Dang X, Chen J, Chen C, Chen Y, et al. Identification of common genes and pathways in eight fibrosis diseases. Front Genet 2020;11:627396.
[32] Vainio LE, Szabó Z, Lin R, Ulvila J, Yrjölä R, Alakoski T, et al. Connective tissue growth factor inhibition enhances cardiac repair and limits fibrosis after myocardial infarction. JACC Basic Transl Sci 2019;4(1):83–94.
[33] Ramazani Y, Knops N, Elmonem MA, Nguyen TQ, Arcolino FO, van den Heuvel L, et al. Connective tissue growth factor (CTGF) from basics to clinics. Matrix Biol 2018;68:44–66.
[34] Fu M, Peng D, Lan T, Wei Y, Wei X. Multifunctional regulatory protein connective tissue growth factor (CTGF): a potential therapeutic target for diverse diseases. Acta Pharm Sin B 2022;12(4):1740–60.